International Journal of analytical and Numerical Methods in Mechanical Design
Winter & Spring 2023 Vol 2 , Issue 1, 57-63

Temperature Analysis of Laser Cladding Process with Mathematical Modelling

Amir Mohammad Sedighi [a,✉], Seyedeh Fatemeh Nabavi [b], Anooshirvan Farshidianfar [c]

[a] Department of Mechanical Engineering, Ferdowsi University of Mashhad, Mashhad, Iran
[b] Reseacher, Department of Mechanical Engineering, Ferdowsi University of Mashhad, Mashhad, Iran
[c] Professor, Department of Mechanical Engineering, Ferdowsi University of Mashhad, Mashhad, Iran

Received 10 April 2023; Revised 15 May 2023; Accepted 20 Juan 2023
✉ amirsedighi.m.e@gmail.com

Abstract

Laser Cladding is one of the processes that is considered in manufacturing of different objects such as airplane blades and shafts. Many studies have been presented to optimize this process, but there is a research gap in the field of temperature simulation effect. The reason for the importance of temperature simulation is the direct correlation of the temperature gradient with the properties of manufactured object. The purpose of this study is to simulate temperature field of laser cladding process with COMSOL6.0 software. After verification of presented temperature with previous study with 0.2 % error, parameter studies including temperature dependent parameters and heat loss are presented verses temperature, time and laser power were presented with mathematical models.

Keywords: Laser cladding, Temperature analysis, parameter studies, heat loss, mathematical modelling

1. Introduction

The laser cladding process is used to create precise and complex shapes in hard-to-machine materials such as Titanium, Ceramics, and Fiber-reinforced composites. Machining with laser beam was considered in the metal plate laser cladding department for the production and repair of parts. Laser cladding is the most widely used due to the flexibility and ease of the system, high precision, machinability of most materials, low noise and creation of a small molten pool. Among the all lasers used in this process, fiber and CO2 lasers are the most used[1].

Layer by layer laser cladding process causes accumulation of high thermal residual stresses. Panda et al.[2] estimated the boundary conditions and the depth of the molten pool with the two-dimensional thermal modeling of cladding with Inconel 718 powder and laser fiber by examining the Marangoni flow, and the maximum temperature of 4440K was obtained. The presented model was able to predict the boundary of the molten pool in the joint part of the coating and the substrate as a function of time, for several parameters of the laser process with acceptable accuracy.

To achieve improved microstructure properties and performance, it is necessary to investigate the solidification mechanism of microstructures formed during laser cladding. Ma et al.[3] simulated solidification in the coating process by combining two Gaussian body heat source and Gaussian zone heat source models with L316 powder, which modeled the part temperature, cooling coefficient, freezing coefficient, and crystal formation mode. By counting grains, it was concluded that the average grain size of the molten pool increases with increasing power.

High energy input and fast cooling rate affect the geometrical morphology and microstructure of laser-cladding aluminum composite coatings. Li et al.[4] experimentally and simulated the freezing behavior and geometry of the molten pool for the first and second layers of coating with AlSiTiNi powder, and the maximum temperature of the first layer was 1973K and the second layer was 2224K, which is the simulation error. In all values, it was estimated between one and eight percent. The maximum temperature gradient was found at the bottom of the melt pool, while the minimum value was at the cladding surface, the maximum solidification rate was at the cladding surface and the minimum value was at the bottom of the melt pool, both of which increased with increasing scanning speed.

The formation of residual stresses caused by the thermal-mechanical effect and microstructural transformation in the laser coating process mainly affects the integrity of the final product and its useful life. Temana et al.[5] modeled four different three-dimensional ellipsoid cases of cladding with two types of Al2O3 and TiC ceramics and with fiber and CO2 lasers on the Ti6Al4V plate, and the highest interference coefficient of TiC ceramic with a fiber laser and Al2O3 ceramics were obtained by CO2 laser. The maximum simulation temperature for the two materials was 4082K and 3170K, respectively. Next, by adding the second pass, the overlap was estimated between 20 and 30 percent. The result of this model is the prediction of temperature distribution, cooling rate, melt pool depth, heat-affected area, and residual stress. This

study mainly highlights the thermal effect on residual stresses for similar and dissimilar cladding/substrate materials and suggests suitable cladding materials with minimum residual stresses.

With the development of software and the addition of different solution methods, the accuracy of the simulation increased day by day and became closer to the laboratory solution, of which the ALE (Arbitrary Lagrangian & Eulerian) method, or the moving mesh, is one of the most common. Parekh et al.[6] modeled the coating with a CO2 laser. By using the ALE technique on the model, the mass was allowed to move inside the part with high deformation, and by applying the remeshing process on the model, the quality of the distorted elements was improved. In this research, they concluded that laser power has a direct relationship with temperature and stress, and the speed of laser movement has a relationship with coating height, temperature stress, and the opposite relationship. On the other hand, with the increase in the diameter of the laser beam, the tension decreased and the dilution and height of the coating increased.

The type of laser radiation is one of the effective parameters that prove this effect. Goffin et al.[7] used wire instead of powder in CO2 laser modeling. In the following, three different types of laser radiation distribution were analyzed experimentally and by simulation, including 1.25mm Gaussian, 3.5mm Gaussian, and 1.25mm base laser beam (the beam collides with the surface of the plate instead of powder) and the maximum temperature in three modes is The order of 3266k, 2085k and 3339k were obtained. Then they concluded that the second model has 31% and the third model has 50% energy savings compared to the first. Therefore, the model of laser radiation on the base metal has the highest energy efficiency.

In this study, we modeled the study of Dada et al.[8] in order to make this modeling closer to reality after confirming the accuracy of the results. In the present study, COMSOL Multiphysics was used to examine the heat transfer mechanism on the steel baseplate during laser deposition of HEAs.

2. Computational analysis

Deposition of the HEA coatings was made on a 40 mm×4 mm baseplate shown in Figure 1 and shown assumptions in Table 1. Global expressions used in the Simulation via COMSOL Multiphysics[8].

The geometry only models the A301 steel and its properties are assumed to be constant. All other boundaries are kept constant except for the boundaries on the top surface. The laser beam's electromagnetic properties are not stimulated; therefore, the effect of its wavelength is not modelled. While changing x0 and y0 can shift the beam's center while the astigmatism and the width of the beam can be controlled through σx σy.

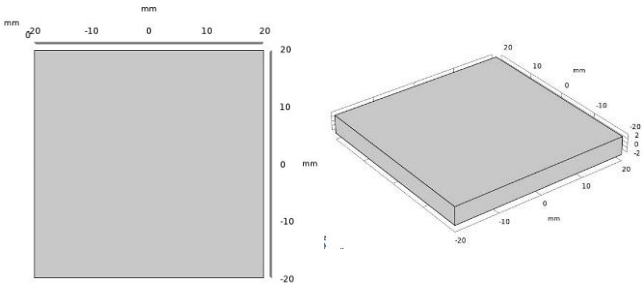

Fig .1. The geometry of the model.

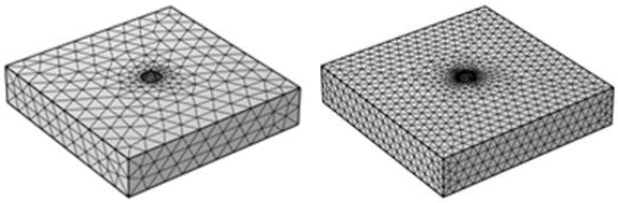

(A) (B)

Fig .2. Mesh; A) Coarse, B) Extra fine.

3. Governing equations and boundary conditions

3.1. Heat equations

The surface of the steel baseplate is dissipated by a laser beam, influenced by radiation and conduction. Gaussian profiles shown in Fig 3 are used to represent the heat source per time. The blue line insert from study [8] and the green line come from this study, then compare

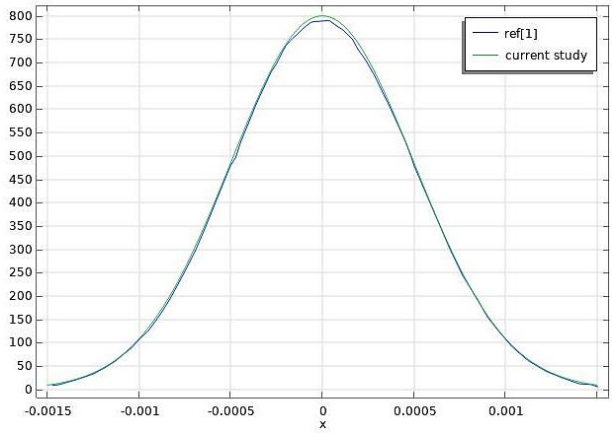

together.

Fig .3. Gaussian Profile of current study and Study.

Table 1
Compare Gaussian Profile of current study and study [8]

Parameter	Value
X	0
Study [8]	800
Current study	788.33
The maximum error of Gaussian profile	1.46%

The time-dependent heat transfer phenomenon is expressed using the following equation (1).

$$\rho C_p \frac{\partial T}{\partial t} + \rho C_p u.\nabla T = \nabla.(k\nabla T) + Q \quad (1)$$

where C is the heat capacity, T is the temperature, k is the thermal conductivity and t is the time. Q is the laser heat, q is the density, and u is the velocity field which is calculated by the mass and momentum conservation equation. The laser deposition process involves a body of heat load in the steel baseplate which is given by equation (2).

$$Q(x,y,z) = SLaser(1-R_c) \times \frac{A_c}{\pi\sigma_x\sigma_y} e^{\frac{(x-x_0)^2}{2\sigma_x^2}+\frac{(y-y_0)^2}{2\sigma_y^2}} .e^{-A_c z} \quad (2)$$

The power input is shown by *SLaser*, the reflection coefficient is shown as R_c, the absorption coefficient is A_c while the Gaussian distribution along the XY-plane is represented in equation (3).

$$e^{\frac{(x-x_0)^2}{2\sigma_x^2}+\frac{(y-y_0)^2}{2\sigma_y^2}} \quad (3)$$

While the exponential decay experienced due to absorption is given as e^{-AcZ} since the planar surface is assumed to be aligned with $z = 0$.

3.2. Analytics and Variables

In this section, we will analyze the study and compare the results of our study with the study[8]. The results are shown in figure 5.

Table 2
Parameter of Analysis 1 insert from Study [8]

Name	Value	Q_{in} (power input)
Expression	exp(-((a-a0)^2/ (2*siga^2)))	S_Laser*(1-Rc)*Ac* (1/(pi*sigx *sigy)) * an1(x, x0, sigx)* an1(y, y0, sigy) *exp(-Ac*abs(z))
Arguments	a, a_0, siga	
Unit	mm, mm, mm	W/m³

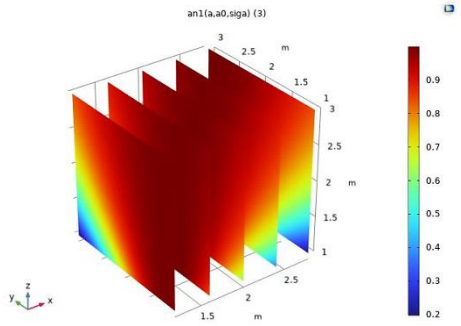

Fig .4. Temperature Slice Plots of the temperature distribution stationary laser with constant power.

3.3. Heat flux

The laser heat source defined as the heat flux across the irradiated surface by the laser beam is the same size as the simulated laser beam which was distributed per time and represented using the Gaussian profile in figure 3.

While the slice plots of the temperature distribution are shown in figure 4. The mathematical function is explained using the heat conduction volume equation (4)

$$\rho C_p \frac{\partial T}{\partial t} - \nabla(k\nabla T) = Gt \quad (4)$$

where steel density is q, C_p is specific heat capacity, k is thermal conductivity, t is time, T is temperature. Heat conduction represents the transfer from the hot to the cold region within the steel plate without macroscopic displacements or considering the work done by pressure changes and viscous dissipation.

This Gaussian model is applied on a This Gaussian model is applied on a hemispherical with a radius of sig$x$=0.3mm sig$y$=0.5mm. The center of this shape is x_0=0.5mm, y_0=0mm and on the upper surface of the screen. Another feature of this circle is the absence of radiation heat transfer. Conduction occurs through the emission of free electrons in the steel when the surface is heated, and the heat then spreads in different directions toward the shape of the hemispherical molten pool, without significant deformation of the geometry.

4. Result and Discussion

4.1. Validation

In this section, we examine the temperature of 4 selected points. In the reviewed study[8], the exact location of the 4 points is not stated and our location is only an estimate.

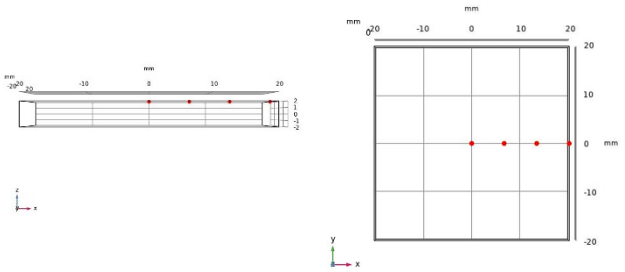

(A) (B)

Fig .5. The 4 points for measure temperature current study A) XZ view B) XY view.

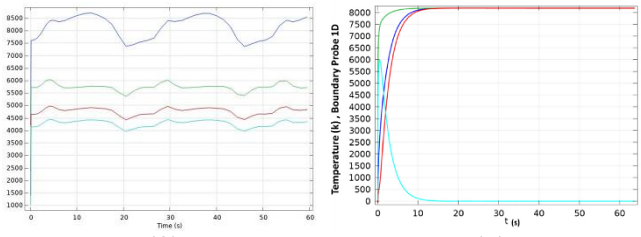

(A) (B)

Fig .6. Time-temperature Probe Plot A) Current study B) Study [8] for stationary laser with constant power

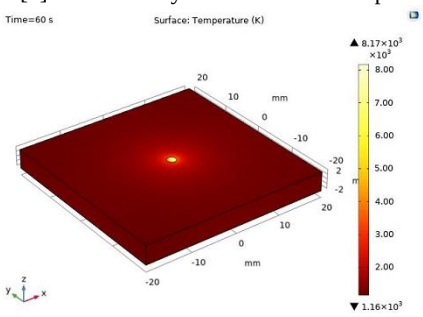

(A)

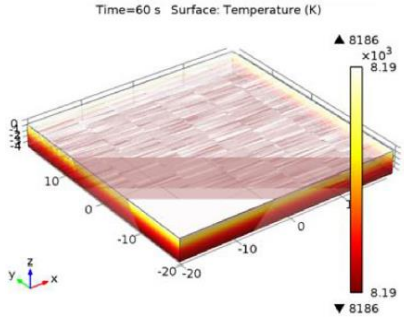

(B)

Fig .7. Time-temperature Probe Plot A) Current study B) Study [8].

Table 3.
Compare current study and Study [8]

Name Study	Hight temp
Study [8]	8186
Current study	8170
Error (%)	0.2%

The temperature in this study was obtained with a 1% error compared to the study [8], the one reason for which is the lack of sufficient information such as the investigated points and some boundary conditions. The second geometry only models the A301 steel and its properties are assumed to be constant.

4.2. Parameter Study: Laser Power

The first parameter is the laser power, the effect of its change on the maximum temperature was investigated.

Table 4.
Laser Power effect on Maximum Temperature

Laser Power [W]	Max Temp [K]
800	4540
1200	6930
1400	7290
1600	8170
1800	9040
2000	9900
2400	11600

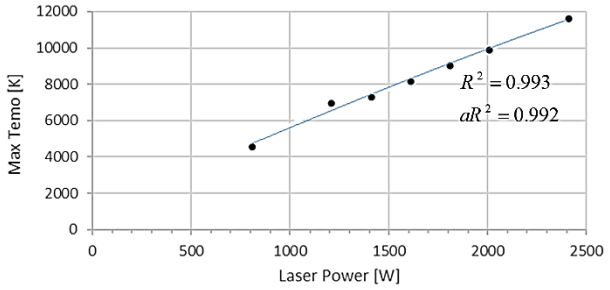

Fig .8. Effect of laser power on maximum temperature.

The table drawn above shows that laser power has a direct and almost linear relationship with the maximum temperature. The governing equation obtained from curve fitting is as follows:

$$T_{\max} = -0.0002P_L^2 + 5.0747P_L + 788.16 \quad (5)$$

4.3. Temperature dependent parameters

In this section, we want to apply 4 temperature-dependent parameters, including density, heat capacity, thermal conductivity, and surface emissivity, then obtain the maximum temperature.

The temperature obtained in the laboratory results is between 1400 and 1600 ^{o}C. The second problem of the reviewed article is the assumption that the properties of the metal are constant in all conditions. The first step is to relate the two properties of thermal conductivity and heat capacity to temperature.

Table 5.
Study [8] and current study

Properties \ Expression	Study [8]	Current study
Density [kg/m^3]	7930	Rho(T)
Heat Capacity [J/(kg.K)]	520	$C_p(T)$
Thermal Conductivity [W/(m.K)]	29	K(T)
Surface Emissivity [1]	0.8	emi(T)

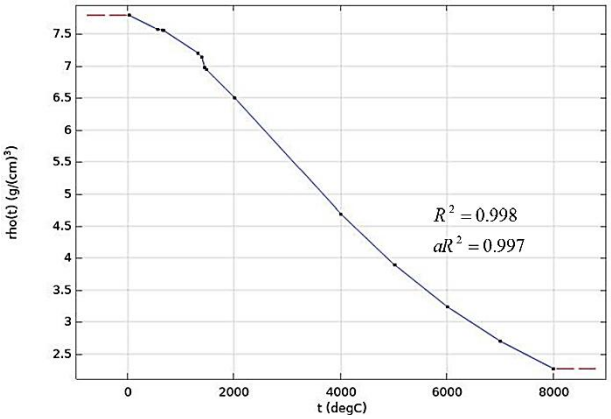

Fig .9. Density per Temperature [rho(T)] JMatpro software.

The curve fitting of the density table with third-order polynomial is as follows:

$$\rho_T = 1E^{-11}T^3 - 1E^{-07}T^2 - 0.0004T + 7.8782 \quad (6)$$

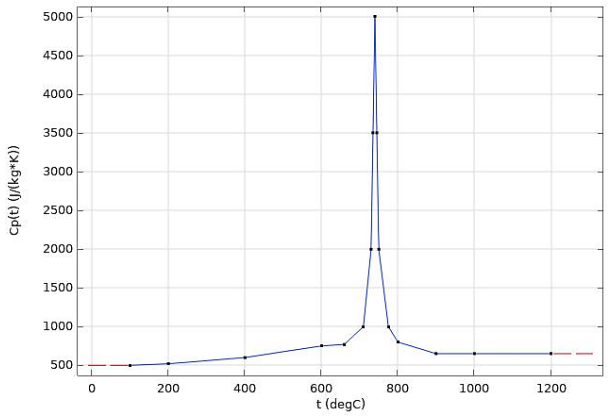

Fig .10. Heat capacity per temperature [Cp(T)].

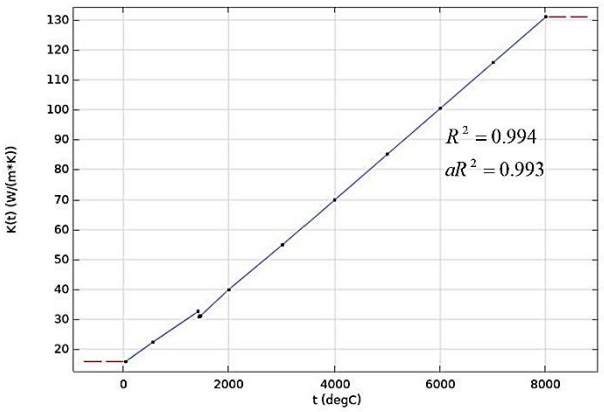

Fig .11. Thermal Conductivity per Temperature [K(T)].

The curve fitting of the thermal conductivity table with second-order polynomial is as follows:

$$K_T = 2E^{-07}T^2 + 0.0129T + 13.544 \quad (7)$$

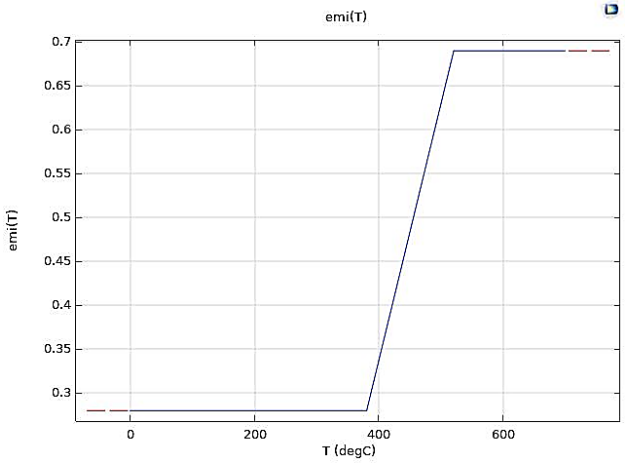

Fig .12. Surface Emissivity per Temperature [emi(T)].

The formula of Surface Emissivity is as follows:

$$\begin{aligned} &T \le 350 \rightarrow \varepsilon = 0.28 \\ &350 \le T \le 520 \rightarrow \varepsilon = 0.00293T - 0.833 \\ &520 \le T \rightarrow \varepsilon = 0.69 \end{aligned} \quad (8)$$

The temperature distribution diagram after applying the changes is as follows.

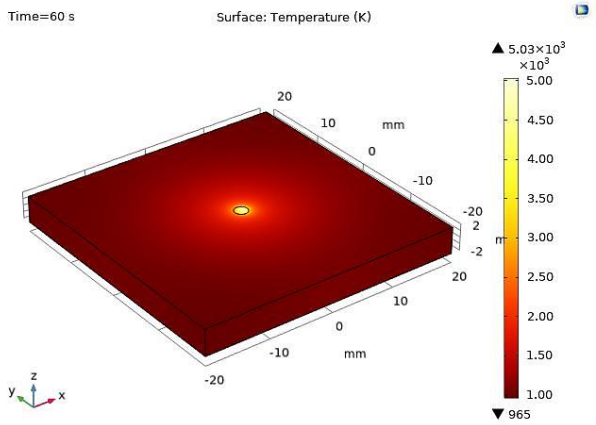

Fig .13. Temperature distribution Plot.

The maximum temperature obtained by applying variable properties to the base metal was 5030 K, which caused a 38.5% decrease in temperature.

4.4. Constant heat conduction

The next important parameter to be investigated is the effect of heat convection on temperature. Next, with some reasonable heat convection coefficients, the maximum temperature is shown in the diagram. T_{ext}=20degC

Table 6.
Heat Convective effect on Maximum Temperature

Heat convection coefficient [W/(m^2.k)]	Max Temp [K]
10	8160
20	8143
30	8127
40	8110

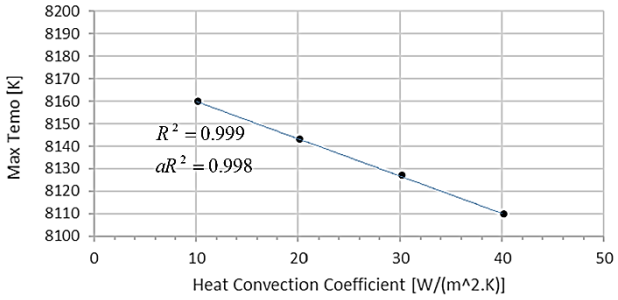

Fig .14. Heat convection effect on maximum temperature.

By adding thermal convection, approximately 0.7% temperature reduction occurs. The governing equation obtained from curve fitting is as follows:

$$T_{max} = -1.66C_{HC} + 8175 \quad (9)$$

4.5. Variable heat convection

In the next heat convection model, the convection coefficient is variable with respect to temperature, which is represented by $h(T)$.

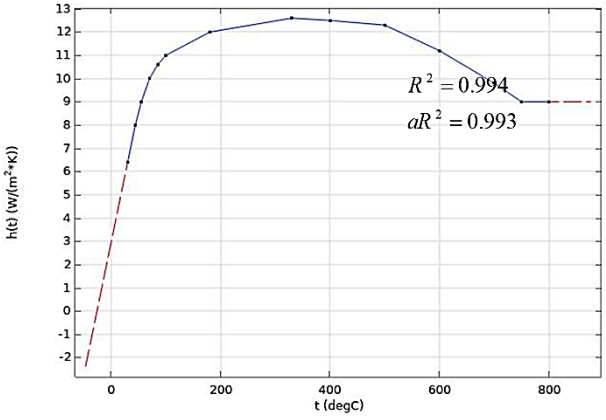

Fig .15. Heat Convection coef. per Temperature [$h(T)$]

The curve fitting of the above table with six-order polynomial is as follows:

$$h(T) = -2E^{-15}T^6 + 7E^{-12}T^5 - 8E^{-09}T^4 + 4E^{-06}T^3 - 0.0012T^2 + 0.1767T + 2.2525 \quad (10)$$

By mixing variable properties and Heat Convection with a coefficient of $h(T)$, the temperature obtained is as follows.

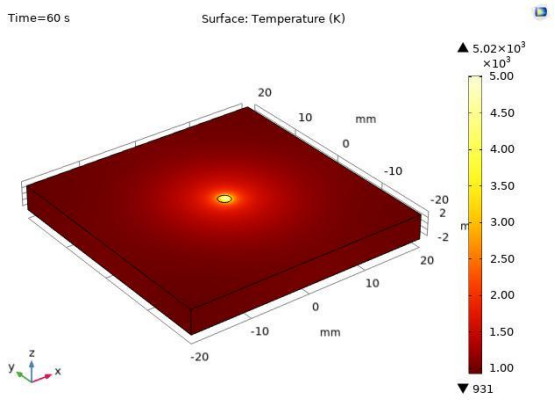

Fig .16. Temperature distribution plot for constant heat convection.

By applying both of the above optimization parameters, the maximum temperature reaches 5020 K, which has reduced the temperature by almost 38.7%.

4.6. Heat loss

This section shows the calculation of heat loss in terms of time according to the maximum temperature of 5020K and the average Temperature of 3700K. The equation is entered in the software as the following formula, where T_{AVE} is the average temperature of the desired circular section.

$$\begin{aligned} hl &= (\sigma\varepsilon_T (T_{AVE}^4 - T_\infty^4) + h_T (T_{AVE} - T_\infty))Area \\ \sigma &= 5.67\times10^{-4} W/(m^2K^4) \\ T_\infty &= 293K \\ Area &= (BeamDiameter/2)^2 \times \pi \end{aligned} \quad (11)$$

In figure 16 shown the heat loss per time, in figure 17 shown heat loss per maximum temperature and in figure 18 shown heat loss per Laser Power. In Figure 16, the heat loss is greatly increased at the beginning, and then the heat loss becomes almost constant as the temperature stabilizes.

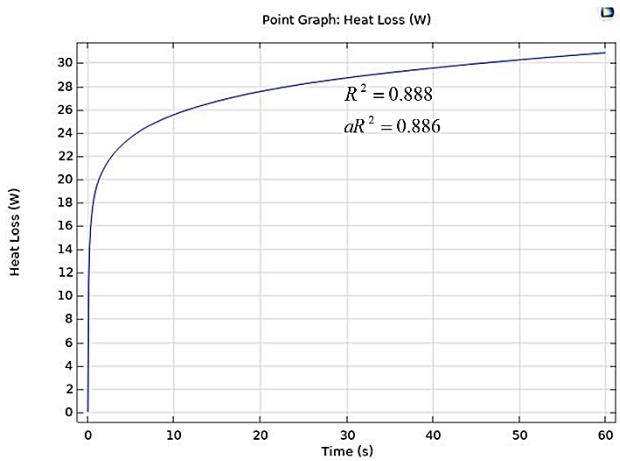

Fig .17. Heat loss per time.

The curve fitting of figure 17 with third-order polynomial is as follows:

$$hl_t = 0.0002t^3 - 0.0189t^2 + 0.7441t + 19.268 \quad (12)$$

In Figure 17, at the beginning and up to the approximate temperature of 2800 K, the heat loss increases linearly because $Emi(T)$ and $h(T)$ are, but after this temperature, the heat loss increases by the order of 3.

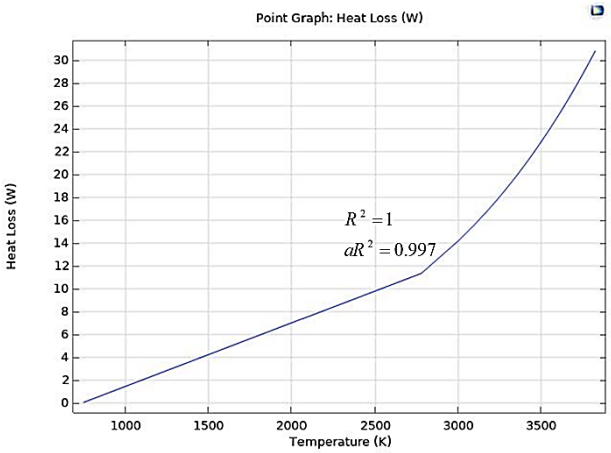

Fig .18. Heat Loss per maximum temperature.

The curve fitting figure 18 of the with third-order polynomial is as follows:

$$hl_T = 1E^{-09}T^3 - 7E^{-06}T^2 + 0.0137T - 7.0888 \quad (13)$$

In Figure 18, heat loss is plotted per laser power, which shows that the behavior is completely linear.

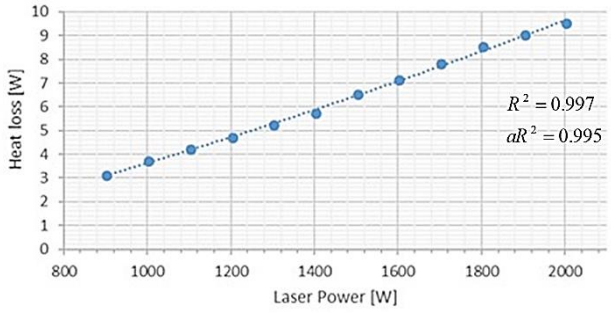

Fig .19. Heat Loss per Laser power in constant temperature of 2000 K.

The curve fitting of the figure 19 with linear as follows:

$$hl_P = 0.006P_L - 2.379 \quad (14)$$

5. Conclusion

In the current study, the temperature field of Laser Cladding process is model considering COMSOL6.0 software. After verification of presented temperature with previous study with 0.2 % error. Presenting mathematical modelling, different results have been conducted. Some of them are as follows:

1. Density is a 3rd order function of temperature with R-squared of 0.998.

2. Maximum temperature is a 2nd order function of laser power with R-squared of 0.993 and a linear function of
3. Thermal Conductivity is a linear function of heat convection coefficient.
4. Heat losses is a third orders functions of time and maximum temperature with R-squared of 0.888 and 1, respectively.
5. The laser power affects of heat losses linearly with R-squared of 0.997.

References

[1] N. Bakhtiyari, Z. Wang, L. Wang, and H. Zheng, "A review on applications of artificial intelligence in modeling and optimization of laser beam machining," Optics & Laser Technology, vol. 135, p. 106721, 2021.

[2] K. Panda, S. Sarkar, and A. K. Nath, "2D thermal model of laser cladding process of Inconel 718," Materials Today: Proceedings, vol. 41, pp. 286-291, 2021.

[3] P. Ma, Y. Wu, P. Zhang, and J. Chen, "Solidification prediction of laser cladding 316L by the finite element simulation," The International Journal of Advanced Manufacturing Technology, vol. 103, no. 1, pp. 957-969, 2019.

[4] Li et al., "Numerical simulation of thermal evolution and solidification behavior of laser cladding AlSiTiNi composite coatings," Coatings, vol. 9, no. 6, p. 391, 2019.

[5] N. Tamanna, I. Kabir, and S. Naher, "Thermo-mechanical modelling to evaluate residual stress and material compatibility of laser cladding process depositing similar and dissimilar material on Ti6Al4V alloy," Thermal Science and Engineering Progress, vol. 31, p. 101283, 2022.

[6] R. Parekh, R. K. Buddu, and R. Patel, "Multiphysics simulation of laser cladding process to study the effect of process parameters on clad geometry," Procedia Technology, vol. 23, pp. 529-536, 2016.

[7] N. Goffin, J. R. Tyrer, L. C. Jones, and R. L. Higginson, "Simulated and experimental analysis of laser beam energy profiles to improve efficiency in wire-fed laser deposition," The International Journal of Advanced Manufacturing Technology, vol. 114, no. 9, pp. 3021-3036, 2021.

[8] M. Dada, P. Popoola, N. Mathe, S. Adeosun, and O. Aramide, "2D numerical model for heat transfer on a laser deposited high entropy alloy baseplate using Comsol Multiphysics," Materials Today: Proceedings, vol. 50, pp. 2541-2546, 2022.